Available online at www.sciencedirect.com
SCIENCE DIRECT®
ELSEVIER
Surface Science 543 (2003) 63–74
SURFACE SCIENCE
www.elsevier.com/locate/susc

Ambient stability of chemically passivated germanium interfaces

D. Bodlaki, H. Yamamoto, D.H. Waldeck, E. Borguet *

Department of Chemistry and Surface Science Center, University of Pittsburgh, 219 Parkman ave., Pittsburgh, PA 15260, USA

Received 18 March 2003; accepted for publication 15 July 2003

Abstract

The stability of any semiconductor surface passivating layer is key to applications. Second harmonic generation (SHG) can be used to probe the chemical state of semiconductor interfaces, as well as investigate the mechanisms of chemical transformation. While the SHG rotational anisotropy changes upon sulfidation or alkylation of Ge surfaces, SHG appears far less sensitive to H and Cl passivation of germanium surfaces than to silicon surfaces. Investigation of the stability of chemically modified germanium surfaces using a number of additional techniques, including atomic force microscopy (AFM) and X-ray photoelectron spectroscopy (XPS), reveals that H- and Cl-terminated Ge(1 1 1) rapidly re-oxidize in ambient. S- and alkyl-terminations are more robust, showing little sign of oxide formation after a month in ambient.
© 2003 Elsevier B.V. All rights reserved.

Keywords: Photoelectron spectroscopy, X-ray photoelectron spectroscopy; Non-linear optical methods; Second harmonic generation methods; Surface chemical reaction; Oxidation; Germanium; Silicon; Sulphides; Single crystal surfaces

1. Introduction

The formation of a stable passivating layer on germanium surfaces is key to applications of this semiconductor material [1]. Germanium is arguably a better semiconductor than silicon, because of its superior carrier transport properties—the mobility of holes and electrons in Ge are more than twice those of Si [2]. Silicon, however, has prevailed because its native oxide is stable whereas germanium's native oxide, GeO_2, is not. In addition, the Ge/GeO_2 interface has a higher trap/surface state density than does Si/SiO_2 [3]. GeO_2 is water soluble further limiting its usefulness. Interest in Ge has renewed because of the ease with which it can be integrated with Si-based devices to fabricate emitters, modulators and receivers for optical communications, e.g., Ge-on-Si near-IR photodetectors [4]. Semiconductor devices based on $Si_{1-x}Ge_x$ alloys are already being commercialized.

Recently, a number of routes to nominally stable termination/passivation layers of germanium have been reported. Notably, wet chemical preparation of H-, Cl-, S- and alkyl-terminations of Ge(1 1 1) and Ge(1 0 0) have been described [5–11]. However, the ambient stability of Cl-, H-, and S-terminated Ge(1 1 1) has not been studied. This is a key parameter for the further use or transformation

* Corresponding author. Tel.: +1-4126248304; fax: +1-4126248611.
E-mail address: borguet@pitt.edu (E. Borguet).

0039-6028/$ - see front matter © 2003 Elsevier B.V. All rights reserved.
doi:10.1016/S0039-6028(03)00958-0

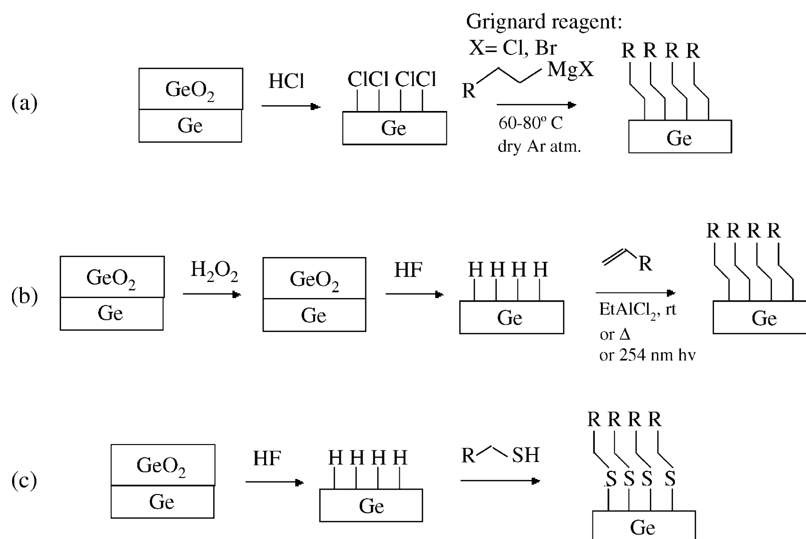

Fig. 1. Alkylation routes of Ge surfaces (a) through Grignard reaction, (b) through hydrogermylation and (c) through reaction with thiols [9–11].

of Ge surfaces, e.g. for the grafting of organic functionality for molecular electronic or sensor applications. Several alkyl-termination schemes for Ge surfaces (Fig. 1) have been reported [9–11]. With Cl-terminated Ge(1 1 1) surface as a starting point, He et al. used a Grignard reagent to attach alkyl monolayers [11]. Choi and Buriak used H-terminated surfaces and a 'hydrogermylation' reaction to alkylate Ge(1 0 0) [9]. Also, grafting of Ge(1 1 1) surface with alkanethiols (octanethiol and octadecanethiol), similar to self-assembly of thiols on Au(1 1 1) surfaces, has been reported [10].

Various analytical techniques, including X-ray photoelectron spectroscopy (XPS), Fourier-transform infra-red spectroscopy (FTIR), Auger electron spectroscopy (AES), high-resolution energy loss spectroscopy (HREELS), contact angle measurements (CA), ellipsometry, and second harmonic generation (SHG) have been employed to study chemically modified semiconductor surfaces [12–18]. SHG studies of chemically modified interfaces are of particular interest since they provide surface sensitivity, probe the electronic response of the interface, and can be carried out in situ. SHG can probe buried interfaces that are difficult to probe by conventional spectroscopic methods [19]. SHG has been used to monitor charge, strain, and microroughness, as well as the progress of chemical reactions on semiconductor interfaces [20–25]. Furthermore, SHG can probe ultrafast electronic processes such as carrier recombination and thermalization [26].

Germanium was one of the first semiconductors to be investigated by surface SHG [27–30]. While the earliest experiments [27] did not report anisotropy in the SHG response with respect to rotation around the azimuthal axis (SHG-RA), later work revealed the presence of strong anisotropy [28]. A detailed phenomenological theory of SHG-rotational anisotropy (SHG-RA) has been developed [31–33]. SHG-RA provides structural and local bonding information at the buried interface [34].

We have investigated the non-linear optical response of chemically passivated germanium surfaces with SHG [35,36]. Combining SHG and XPS, the stability of these surfaces in ambient was investigated. We show that the SHG rotational anisotropy changes upon chemical modification of the Ge surface as well as investigate the mechanisms of these changes.

2. Experimental

2.1. Sample preparation

Ge(1 1 1) wafers (undoped, Eagle Picher) were degreased by successive 10-min sonications in trichloroethylene (J.T. Baker reagent grade), acetone (EM Science, reagent grade), then methanol (Fisher Scientific, Certified ACS grade). No additional treatment was performed on oxidized samples before experiments. All chemicals were purchased from Aldrich Co., unless otherwise stated, and used as received.

Although different protocols were used to prepare the different modified surfaces, each one began with an oxidized Ge surface (see Fig. 1). For chemical modification, the clean, oxidized Ge samples were hydrogen-terminated by dipping in 48% HF (Mallinckrodt, reagent grade) five times for 10 s, each time followed by a 20 s rinse in ultrapure (>18 MΩ·cm) water. Finally, the sample was dried in N_2 gas [5].

Clean, oxidized Ge samples were chloride-terminated by dipping in diluted (10%) HCl for 10 min [6]. Then the sample was briefly (<5 s) rinsed in ultrapure water and blown dry with N_2.

Alkylated Ge was prepared by the halogenation/alkylation procedure employed for Si(1 1 1) [13]. After hydrogen-termination, the Ge sample was exposed to a solution of PCl_5 in deoxygenated chlorobenzene using benzoyl peroxide as a radical initiator, in a flask under Ar (99.99%), and gently warmed for 30 min. Following removal of the chlorobenzene solution, the sample was rinsed with fresh, deoxygenated chlorobenzene, while still in the flask and under Ar. Once the chlorobenzene was completely removed, decylmagnesium bromide (1 M in ether) was introduced into the flask and allowed to react at room temperature for 24 h. After the reaction was complete, the sample was rinsed with anhydrous ether and sonicated for 10 min each in methanol then dichloromethane.

Sulfidation of the Ge(1 1 1) surface was achieved by immersion of hydrogen-terminated Ge in $(NH_4)_2S$ at 70 °C for 20 min then rinsing in MeOH and drying by N_2 flow [7,8]. The structure of the resulting overlayer, i.e., a monolayer of bridge-bonded S atoms [7] vs. several layers of amorphous GeS_x [8] is still debated thus we will refer to this surface as Ge–S or sulfur-terminated Ge.

2.2. Second harmonic generation rotational anisotropy

Second harmonic generation rotational anisotropy measurements were carried out to control the exactness of the crystal cut and the effects of wet chemical treatment. In these experiments, the azimuthal angle, ϕ, was measured with respect to the $[2\bar{1}\bar{1}]$ direction. SHG measurements were carried out with 4 ps pulses from a Ti:sapphire regenerative amplifier operating at 1 kHz [37]. The *p*-polarized 800 nm beam was incident on the sample at 45° with respect to the surface normal. The fluence was typically 0.01 J/cm^2. The beam was optically filtered (Kopp Glass #2-63) to remove second harmonic photons (400 nm) and lightly focused to a beam diameter, determined using a knife edge technique, of 1.1 ± 0.1 mm. The beam area was corrected for elliptical shape obtained at non-normal incidence. The reflected beam was sent to a monochromator (Acton Research, 300i, 2400 gr/mm grating) after short-pass filtering (Kopp Glass #4-94) to block 800 nm photons. A liquid nitrogen cooled CCD camera (Princeton Instrument, CCD30-11) was used in single element detection mode. An analyzing polarizer was set to pass either *s*- or *p*-polarized SH photons. The quadratic nature of the second harmonic response was verified in the power range explored [38]. The SHG response was normalized to the SHG signal from the native oxide sample at the azimuth of maximum SHG ($\phi = 0°$).

2.3. X-ray photoelectron spectroscopy (XPS)

X-ray photoelectron spectra were obtained on a Physical Electronics model 550 apparatus [39]. A cylindrical, double-pass analyzer analyzed the energy of the photoelectrons. The analyzer was apertured to restrict the acceptance angle to ±6° [39]. The energy resolution of the apparatus was determined to be 1 eV [39]. X-ray photoelectron spectra were taken using an AlKα X-ray source (1486.3 eV) and all the spectra were taken at 30°

take-off angle. The pressure in the analytical chamber was $\sim 10^{-9}$ Torr during analysis. Spectra of C(1s) (binding energy, B.E. 280–290 eV), Ge(2p) (B.E. ~1215–1225 eV), Ge(3d) (B.E. ~25–35 eV), O(1s) (B.E. ~526–536 eV), F(1s) (B.E. ~675–689 eV), Cl(2p) (B.E. ~188–204 eV) were collected.

2.4. Atomic force microscope (AFM)

AFM images were acquired with a Dimension 3100 microscope (Digital Instrument) in contact mode using a Si_3N_4 tip with 0.12 N/m spring constant.

3. Results and discussion

3.1. SHG-RA

H- and Cl-termination of Si(1 1 1) surfaces induces a change in the surface electronic properties and the non-linear optical (SHG) response [24]. Likewise the chemical modification of the Ge(1 1 1) surface, stripping off the oxide and replacement by a monolayer of H, Cl, alkyl or S, should alter the non-linear optical properties of the interfaces. The SHG rotational anisotropy of native oxide, hydrogen-, chloride-, decyl- and sulfide-terminated Ge(1 1 1) surfaces in air at 800 nm fundamental wavelength are shown in Fig. 2 for the p_{in}/p_{out} polarization combination. The p_{in}/p_{out} rotational anisotropy patterns show threefold symmetry with three small and three large peaks separated by 120° and a weak isotropic offset from the background.

The phenomenological theory of SHG-RA provides a framework for understanding these patterns [31–33]. The rotational anisotropy in the p_{in}/p_{out} polarization combination may be described by

$$\frac{I_{pp}(2\omega)}{(I_p(\omega))^2} \sim |A_{pp} + B_{pp}\cos(3\phi)|^2 = |A_{pp}|^2 + |B_{pp}|^2\cos^2(3\phi) + 2|A_{pp}| * |B_{pp}|\cos(3\phi)\cos(\Delta_{AB}) \quad (1)$$

where ϕ is the azimuthal angle measured between the plane of incidence and the $[2\bar{1}\bar{1}]$ direction of

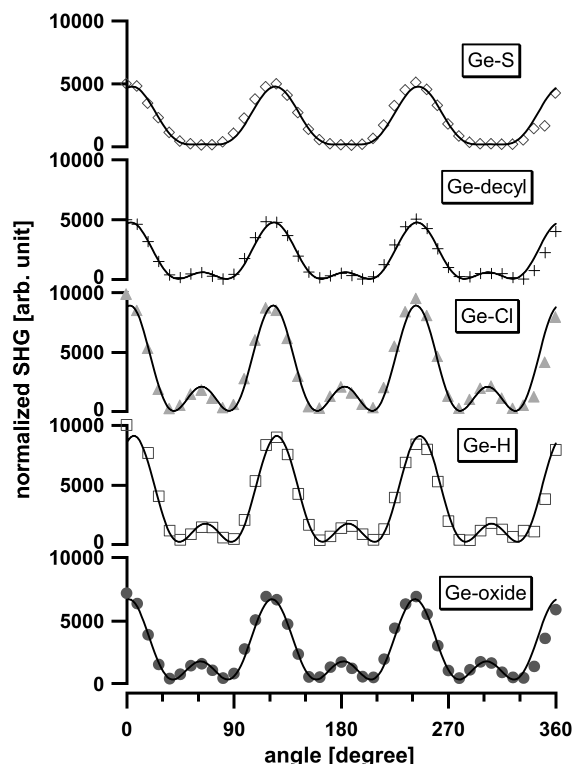

Fig. 2. SHG-RA of variously terminated Ge(1 1 1) surfaces in air: natively oxidized (●), hydrogen- (□), chloride- (▲), decyl- (+) and sulfide-terminated (◇) Ge(1 1 1). All the SHG-RAs were taken in the p_{in}/p_{out} polarization combination at 800 nm fundamental wavelength. The solid lines are fits using Eq. (1).

the single crystal [35]. A_{pp}, the isotropic contribution, and B_{pp}, the anisotropic contribution, are specific to the p_{in}/p_{out} polarization combination. A_{pp} and B_{pp} depend on the non-linear coefficients, the angle of incidence, and the linear optical properties of the interface at the fundamental and second harmonic wavelengths [35]. A_{pp} and B_{pp} are complex and have a relative phase Δ_{AB} defined by

$$\frac{B_{pp}}{A_{pp}} = \frac{|B_{pp}|}{|A_{pp}|}\exp(-i\Delta_{AB}) \quad (2)$$

The parameters $|A_{pp}|$, $|B_{pp}|$ and Δ_{AB} obtained from the fit to the data are shown in Table 1. These values, particularly the $|B_{pp}|/|A_{pp}|$ ratio and Δ_{AB}, are used to evaluate the effect of chemical modification on the non-linear optical response.

Table 1
SHG rotational anisotropy parameters of Ge(1 1 1)–GeO_2, Ge(1 1 1)–H, Ge(1 1 1)–Cl, Ge(1 1 1)–decyl and Ge(1 1 1)–S surfaces in the p_{in}/p_{out} polarization combination at 800 nm

p_{in}/p_{out}	Ge(1 1 1)–GeO_2	Ge(1 1 1)–H	Ge(1 1 1)–Cl	Ge(1 1 1)–decyl	Ge(1 1 1)–S
A_{pp}	31	36	30	26	36
B_{pp}	63	65	69	46	36
B_{pp}/A_{pp}	2 ± 0.3	1.8	2.3	1.8	1
Δ_{AB}	53 ± 10	34	29	21	20
$\left[\left(\frac{B_{pp}}{A_{pp}}\right) - \cos\Delta\right]^2$	1.95	0.94	2.03	0.75	0.004

A_{pp}, B_{pp}, ratio of A_{pp} and B_{pp}, and their relative phase Δ_{AB} were obtained by fitting the SHG-RA pattern in Fig. 2 using Eq. (1).

One would expect the greatest change upon chemical modification to occur in the p_{in}/p_{out} polarization combination SHG-RA, as was found for both Ge(1 1 1) and Si(1 1 1) [24,35]. Only the p_{in}/p_{out} polarization combination contains the non-linear susceptibility component describing the polarization perpendicular to the interface referred to as ∂_{33} [24,35]. If the non-linear response of the surface changes because of modification of the dipole of the terminating Ge surface bonds, the ∂_{33} component is expected to change. H- and Cl-termination of Ge(1 1 1) results in far less pronounced changes in the p_{in}/p_{out} polarization combination SHG-RA than H- and Cl-termination of Si, however [24]. For the H-termination of Si(1 1 1) a phase shift of about 150° was observed [24], whereas only a slight decrease in the phase shift is found for Cl- and H-termination (see Table 1). The slight increase in B_{pp} is in accordance with the increase of the overall SHG-RA signal magnitude compared to the Ge/GeO_2 interface (see Table 1 and Fig. 2). On the other hand, the changes were more pronounced in the s_{in}/p_{out} polarization combination for these surfaces (not shown). The ∂_{33} component is absent in the s_{in}/p_{out} polarization combination. The non-linear components s_{in}/p_{out} polarization combination (∂_{11} and ∂_{31}) reflect a change in the surface 'backbonds' [35]. Assuming that surfaces are indeed oxide-free and terminated by Cl and H respectively, it would appear that chemical modification by these species affects the 'backbonds' more than the bonds normal to the surface.

The decyl- and S-termination affect the non-linear response in the p_{in}/p_{out} polarization combination to a greater extent than does the H- and Cl-termination. The magnitude of the small peaks and the overall signal decreased as the surface termination changed from oxide to alkyl to sulfide (Fig. 2). The decrease of the B_{pp}/A_{pp} ratio and the phase Δ_{AB} reflects the decrease in the magnitude of the small peaks, while the decrease in the magnitude of the B_{pp} coefficient reflects the decrease in the overall signal (Table 1). More quantitatively, the amplitude of the small peaks with respect to the minimum signal is given by $[(B_{pp}/A_{pp}) - \cos\Delta]^2$.

The observed trends can be understood by considering the Ge(1 1 1) interface as a network of terminated surface bonds. The surface bonds, as well as the Ge–Ge backbonds, may be polarized by chemical bonding at the interface [24]. The polarization of the surface bonds should increase the SHG response as noticed in SHG experiments on Si(1 0 0) with variable H-coverage in UHV—saturation of silicon dangling bond with hydrogen quenched the SHG response [40]. In addition, strain at the interface arising from lattice mismatch between the oxide and the substrate can affect the SHG [41].

In the light of previous second harmonic generation studies at Si(1 1 1) [24] and Ge(1 1 1) [35] surfaces, the rotational anisotropy of Ge(1 1 1)–H and Ge(1 1 1)–Cl at 800 nm are surprising. The trends in the non-linear susceptibility coefficients at the Si(1 1 1)–SiO_2, –H, and –Cl surfaces suggest that surface bond polarity is correlated to the magnitude of the rotational anisotropy [24]. Electronegativity differences ($\Delta\chi$ of 1.43 for GeO, 1.15 for GeCl, 0.54 for GeC and 0.57 for GeS and 0.19 for GeH) provide a measure of the polarity of a bond between two atoms [42]. Consequently, with the Ge–O bonds being most polar, and the polarity

of Ge–H bond being least polar, the rotational anisotropy patterns were expected to change the most from the oxidized to the hydrogen-terminated surface as observed for the Si(1 1 1) surfaces [24]. The small change in the rotational anisotropy between the Ge(1 1 1)GeO_2 and Ge(1 1 1)–Cl, is consistent with this similar electronegativity difference. For decyl- and sulfur-terminated Ge, the rotational anisotropy patterns changes are consistent with the electronegativity differences of decyl– and sulfur–Ge(1 1 1). Although an even greater change is expected in the SHG-RA pattern of H-terminated Ge, i.e. change in the phase or decrease in the overall signal magnitude, than for decyl–Ge or S–Ge this was not observed.

The lack of significant change in the SHG-RA pattern for Ge(1 1 1)–H may indicate incomplete (i.e., defective or inhomogeneous) H-termination of the surface. SHG-RA at 800 nm is a sensitive probe of the electronic properties at the H–Si(1 1 1) surface [43,44]. A complete H monolayer on Si(1 1 1) is characterized by a phase of 150–170° in the p_{in}/p_{out} polarization combination. Incomplete or partially oxidized H monolayers lead to values of Δ_{AB}, less than 150° [44]. Incomplete H- and Cl-termination can be the result of instability of the Ge(1 1 1)–H and Ge(1 1 1)–Cl surfaces in air. We found previously that Si(1 1 1)–H undergoes oxidation in ambient and that photons accelerate the oxidation [43,44]. The same process may occur for the Ge(1 1 1) surface. Therefore, not only the degree of oxide removal but also the stability of the H–Ge(1 1 1) and Cl–Ge(1 1 1) surface to ambient oxidation was investigated.

3.2. XPS

The quality and stability of H- and Cl-terminated Ge(1 1 1) surfaces can be monitored by a complimentary probe, X-ray photoelectron spectroscopy (XPS). The Ge(2p) region of the XPS spectrum is commonly used to follow the removal of the oxide layer and surface derivatization because of its sensitivity to the different oxidation states of germanium [5,6,45]. The Ge(2p) band is also more surface sensitive than the Ge(3d) band because of the smaller mean free path associated with the Ge(2p) core level photoelectrons in the 200–300 eV kinetic energy range [5]. The Ge(1 1 1)–GeO_2 interface has two characteristic peaks in the Ge(2p) band. The low-energy peak (at 1217.9 eV binding energy) is attributed to the presence of elemental Ge [45]. The high-energy peak (at 1220.6 eV) is caused by the +4 oxidation state of Ge which is bound to oxygen [45]. The peak from suboxide species, GeO_x ($x < 2$) has been reported at 1219 eV [45]. The native oxide spectrum (Fig. 3) was fit with these three peaks and indicates that the native oxide is primarily GeO_2 but has a non-negligible suboxide contribution. It is especially important to consider the peak from the suboxide species when the oxide removal is judged from the Ge(2p) region. The GeO_x peak can be obscured by the more intense elemental Ge signal, making the surface appear to be oxide-free. Therefore, the ability to fit the elemental Ge peak with a single peak should be the criterion for complete oxide removal. Recording the signal from the O(1s) core level can further confirm the presence or absence of the oxide.

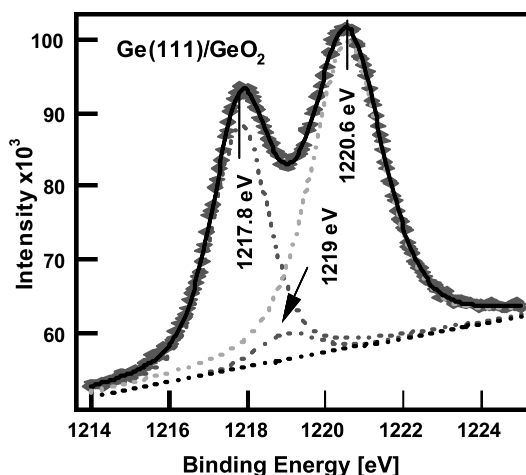

Fig. 3. XPS spectra of Ge(1 1 1)–GeO_2 interface in the Ge($2p_{3/2}$) region. Diamonds indicate the experimental points. The fitted peaks associated with the elemental Ge, Ge in the +2 and Ge in the +4 oxidation state are shown as dashed lines. The dashed black line indicates the baseline, while the solid black line indicates the sum of the fits to the peaks and the baseline. Mixed Gaussian–Lorentzian peak shape was used to fit the spectra.

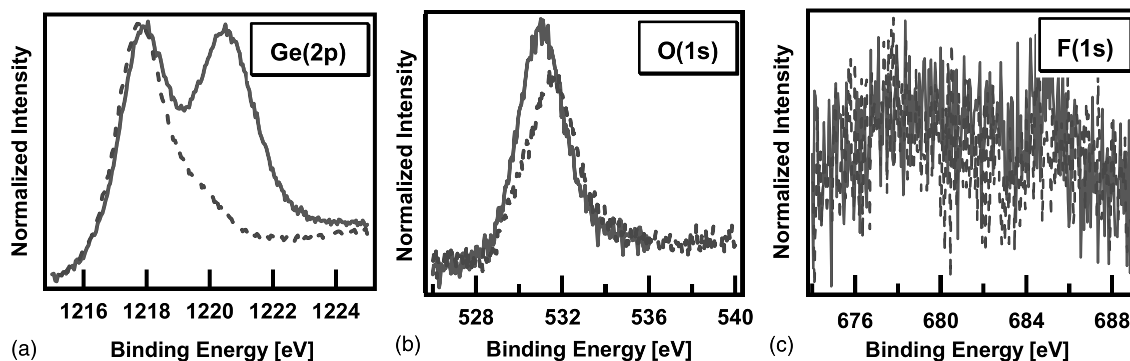

Fig. 4. X-ray photoelectron spectra of HF treated Ge(1 1 1). The Ge($2p_{3/2}$) (a), O(1s) (b), and F(1s) (c) spectral regions are shown. The solid line indicate the spectra of Ge(1 1 1)–GeO_2. The dashed line is the spectra of Ge(1 1 1) after alternating immersion in HF (10 s) and DI water (20 s) repeated five times. The samples were inserted to the load lock immediately (1–2 min) after treatment.

The XPS spectrum of the HF treated Ge(1 1 1) shows the disappearance of the oxide peak at 1220.6 eV (Fig. 4). However, the remaining elemental Ge peak cannot be fit with a single peak, but has a shoulder centered around 1219.3 eV. The shoulder is consistent with the presence of suboxide, GeO_x on the surface and indicates that the removal of the oxide is not complete. The presence of the O(1s) peak further confirms that some oxide is still present at the surface (Fig. 4b). Oxide may remain after etching; or it may grow during rinsing and the 2 min between rinsing and vacuum pump down. A lack of a F(1s) peak confirms that the terminating species, if any, is not F (Fig. 4c).

The XPS data is consistent with the assumption that the H monolayer is incomplete. Less than a monolayer of suboxide can be the source of the smaller change in SHG-RA pattern upon HF treatment, compared with Si. An XPS study of H-termination and stability of H-terminated Ge(1 1 1) and (1 0 0) reported total removal of the native oxide using the alternating HF/H_2O treatment [5]. Even though the procedure described by Deegan and Hughes to prepare Ge(1 1 1)–H was followed, we did not achieve total removal of oxide. It should be noted that the HF grade in this procedure (Mallinckrodt, reagent grade) and theirs (LSI 1 class) is different [5]. It is also possible that the short (five times repeated 10 s) HF dip is not sufficient to form a uniform H monolayer. Choi and Buriak showed that immersion in HF for 10 min was necessary to achieve the best H-termination on Ge [9]. Though Choi and Buriak did not report on the surface's stability, it was sufficient for the acquisition of an FTIR spectrum. Nevertheless, this H-termination of Ge(1 1 1) was successful enough as a first step in grafting decyl onto Ge(1 1 1) [35]. As is shown later, a Ge(1 1 1)–decyl surface is formed in that procedure and is resistant to oxidation for over a month (Fig. 9). It may be that the H-terminated surface was slightly oxidized during insertion of the sample to the load lock (∼1–2 min), because of its the instability in air. Similarly, the SHG-RA measurement is taken in air and requires about 5 min to set up. In contrast, the insertion of the sample to the Schlenk line during the alkylation procedure takes only a few seconds, possibly leading to less oxidation of the surface.

The Cl-termination of Ge(1 1 1) was investigated by XPS, Fig. 5. The disappearance of the high-energy peak in the Ge(2p) region indicates that the oxide is removed. A single peak fits the elemental Ge peak, showing that suboxides are removed as well. The O(1s) peak was absent following the treatment (Fig. 5b). Further evidence of the Cl-termination is the presence of a Cl(2p) feature (Fig. 5c) [6]. However, the Cl-terminated Ge(1 1 1) surfaces and the H-terminated surfaces are unstable in air. The X-ray photoelectron spectra (Fig. 6) of the same samples of H–Ge(1 1 1) and Cl–Ge(1 1 1) immediately following preparation and after storage in air for one hour, one day, one week, one month show the growth of the

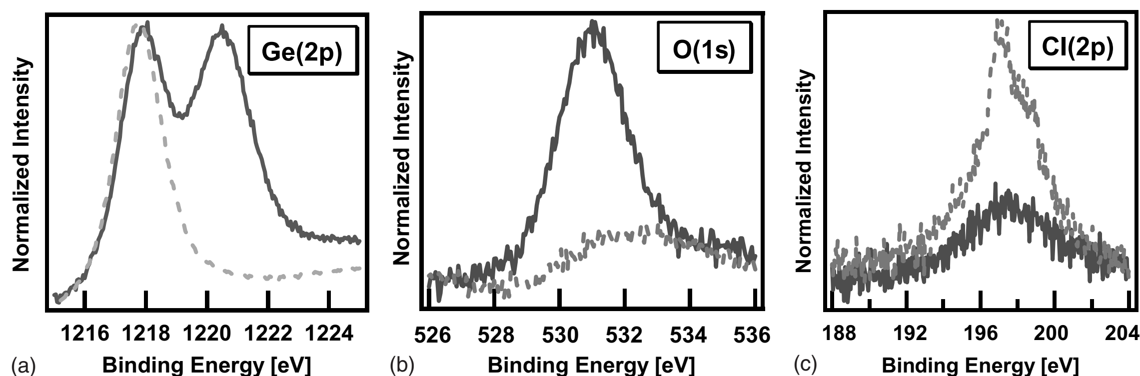

Fig. 5. X-ray photoelectron spectra of Ge(1 1 1)–Cl. The Ge($2p_{3/2}$) (a), O(1s) (b), and Cl(2p) (c) spectral regions are shown. The solid line indicate the spectra of Ge(1 1 1)–GeO_2. The dashed line is the spectra of Ge(1 1 1) after immersion in HCl for 10 min. The samples were inserted to the load lock immediately (1–2 min) after treatment.

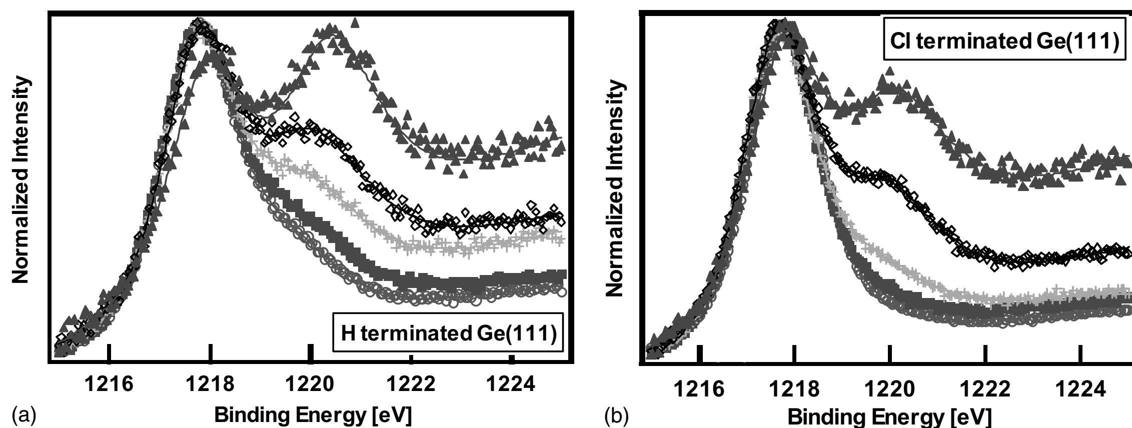

Fig. 6. Oxidation of H- and Cl-terminated Ge(1 1 1). XPS spectra (a) H-terminated Ge(1 1 1) and (b) Cl-terminated Ge(1 1 1) immediately after preparation (○), and after 1 h (■), 1 day (+), 1 week (◇), 1 month (▲) air exposure.

Ge(2p) peak characteristic of the presence of the oxide (GeO_x) peak and corresponding growth of the O(1s) peak for both surfaces (not shown). In addition, the intensity of the Cl(2p) signal decreases and disappears at the Ge(1 1 1)–Cl surface (not shown).

The thickness of the oxide layer present on the HF and HCl etched samples left in air was estimated from the comparison of the intensity ratios of the substrate (I_{sub}) and the oxide (I_{ox}) peaks for the Ge($2p_{3/2}$) core levels [5,46,47]. When two chemical states of the same element, one in the overlayer and one in the substrate, are present the thickness of the overlayer, d, can be calculated by

$$d = \lambda \cdot \cos\theta \cdot \ln\left(\frac{I_{ox} I_{sub}^{\infty}}{I_{sub} I_{ox}^{\infty}} + 1\right) \tag{3}$$

where λ is the attenuation length, θ is the angle between the surface normal and the emission direction, I_{ox}^{∞} and I_{sub}^{∞} are the intensity of the photo emission core level peak of an infinitely thick oxide sample and an oxide-free germanium sample, respectively [47]. The two chemical states of germanium (I_{ox} and I_{sub}) are the elemental germanium in the substrate (1217.9 eV) and the germanium in +2 (1219 eV) and +4 (1220.6 eV) oxidation states in the GeO_x ($x \leqslant 2$) matrix. We estimated the value of I_{sub}^{∞} and I_{ox}^{∞} from the intensity of the Ge^0(2p) peak

in the spectrum of the freshly prepared, oxide-free Ge(1 1 1)–Cl [1] and from the intensity of the Ge^{4+}(2p) peak in the spectrum of the Ge(1 1 1)–native oxide sample. We used the previously published value of the 0.9 nm for the escape depth [5]. The angle between the surface normal and the emission direction, θ, is 30° in these experiments.

The above calculation indicates that a 5 Å oxide covers the HF treated Ge(1 1 1) immediately after preparation in accordance with the presence of the O(1s) peak in the XPS spectrum of freshly prepared 'Ge(1 1 1)–H' (Figs. 4 and 7). In contrast, Deegan and Hughes reported that a 3 Å oxide is grown after two days [5]. The Cl-terminated Ge(1 1 1) is oxide-free up to an hour (Fig. 7). Both samples show a logarithmic increase of the oxide thickness with time. Archer has investigated oxidation of HF treated Ge by ellipsometry and found that oxide growth follows a logarithmic law [48]. The rate of oxide growth was determined to be 0.07 nm/decade for Ge(1 1 1)–H and 0.14 nm/decade for Ge(1 1 1)–Cl. Interestingly, after an initial period, the growth of the oxide seems to be faster for Ge(1 1 1)–Cl than for Ge(1 1 1)–H (Fig. 7).

It is also interesting to compare the oxidation of Ge(1 1 1)–H and Ge(1 1 1)–Cl to the oxidation of H–Si(1 1 1). At the Si(1 1 1)–H surface, a slow oxygen uptake ('induction period') is followed by a fast, logarithmic oxide growth [46,49,50]. The onset of the fast oxide uptake was connected to an oxygen coverage of ~0.7 ML [46,51]. No initial slow oxidation was observed at the Ge(1 1 1)–H surface which could be explained by the presence of greater than a monolayer of oxygen on the surface at the start of the measurement. In contrast, the Ge–Cl surface showed no apparent oxidation for an hour (Fig. 7). It seems, that Ge–Cl is more resistant to oxidation than Ge–H, in accordance with the relative strength of the bonds [6]. But even Ge(1 1 1)–Cl is a far less passivated surface than Si(1 1 1)–H where the slow oxidation and

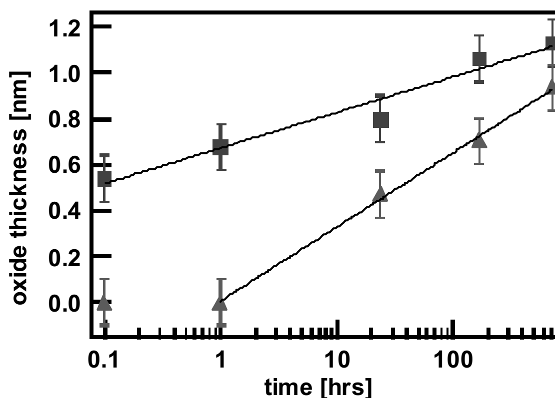

Fig. 7. Oxide thickness on the HF (■) and HCl-treated (▲) Ge(1 1 1) surfaces as a function of exposure to air. The oxide thickness was estimated using Eq. (3) from the data in Fig. 6. The solid lines are logarithmic fits ($y = a * \ln(x) + b$) on the data points.

build up of a monolayer of oxide (~3 Å) can take as long as 15–20 days [46,51].

On the contrary, the stability of the S- and decyl-terminated surfaces is quite remarkable. The SHG-RA of the Ge(1 1 1)–S freshly prepared and after exposure to air for 6 and for 62 days are shown in Fig. 8b. After two months a slight increase in the magnitude of the small peak is observed. It is accompanied by a slight increase in the B_{pp}/A_{pp} ratio from 1 to 1.6 and in the phase, Δ_{AB}, 20 to 26. Han et al. pointed out that alkyl layers attached to the Ge surface through S are not as stable as the Au–S and Ge–C linkages [10]. The authors observed no change in contact angle exposing the Ge–S–alkyl to air for 12 h, but after one-day exposure the contact angle decreased from 101° to 90° [10]. However, in comparison to the H- or Cl-termination, the S-terminated Ge(1 1 1) showed remarkable stability on a few days time scale. A further advantage of the S–Ge(1 1 1) surface is that the sulfide-termination leads to a flat surface that has a surface roughness comparable to that of the chemically cleaned GeO_2 (AFM images not shown) in agreement with previous reports [7].

Covalently bonded organic monolayers on semiconductor surfaces are built with potential biosensor and microelectronics applications in mind where the thermal, chemical and air stability

[1] Ideally an adsorbate free Ge(1 1 1) surface would be used. The fresh Ge(1 1 1)–Cl provides the next best approximation.

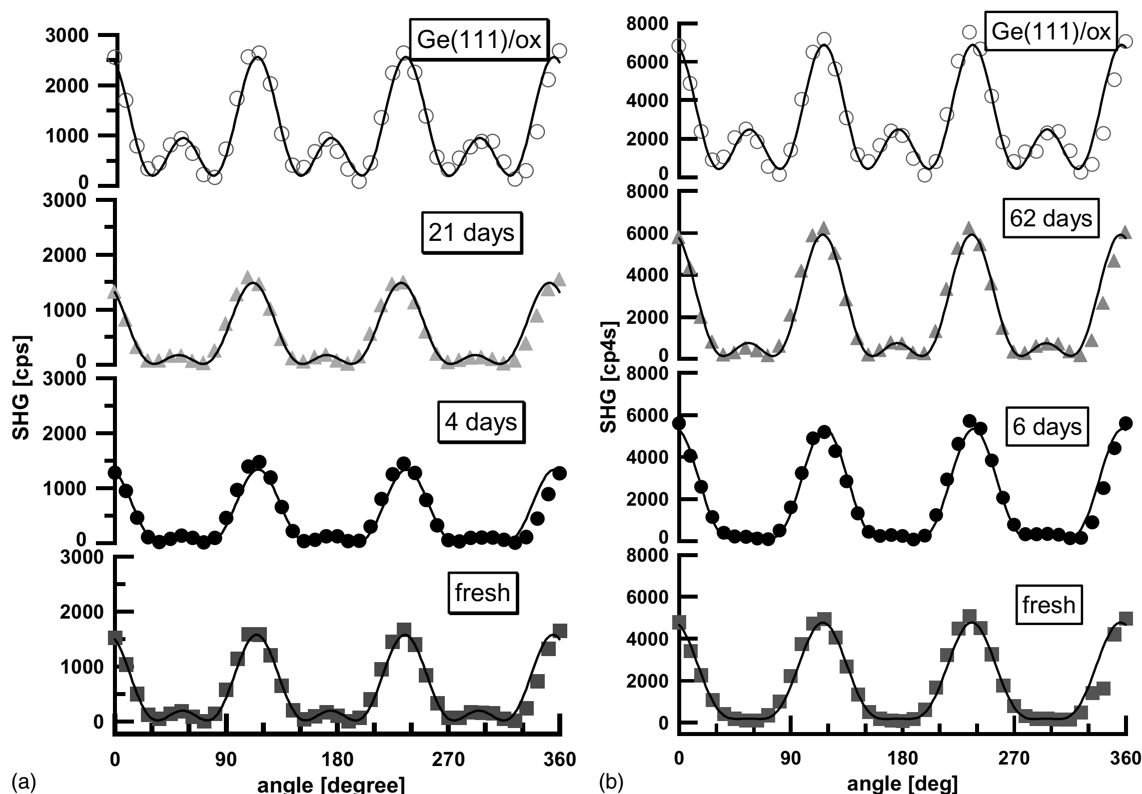

Fig. 8. Stability of Ge(1 1 1)–decyl (a) and Ge(1 1 1)–S (b). The SHG-RA of Ge(1 1 1)–GeO_2 (○) and Ge(1 1 1)–decyl immediately (■), 4 days (●), and 21 days (▲) after preparation. The SHG-RA of Ge(1 1 1)–GeO_2 and Ge(1 1 1)–S immediately (■), 6 days (●), 62 days (▲) after preparation. All the SHG-RAs were taken in the p_{in}/p_{out} polarization combination at 800 nm fundamental wavelength.

is an important question. Alkyl monolayers prepared by the Grignard reaction were found to be air stable up to five days. [11] Alkanethiol monolayers prepared by the thiol attachment chemistry were less resistant, being air stable only up to 12 h [10]. The rotational anisotropy of the Ge(1 1 1)–alkyl, taken after storage in air for 4 and 21 days (Fig. 8a), show no change, i.e. the value of B_{pp}/A_{pp} and their phase Δ_{AB} remain constant within experimental error. This observation suggests the decyl-terminated Ge(1 1 1) is stable in air for at least several weeks. The absence of the characteristic oxide peak in XPS measurements, performed on samples exposed to ambient for four weeks (Fig. 9), supports the findings of the SHG-RA measurement. The shoulder on the elemental Ge peak indicates the presence of suboxide. This suboxide must have formed during preparation of

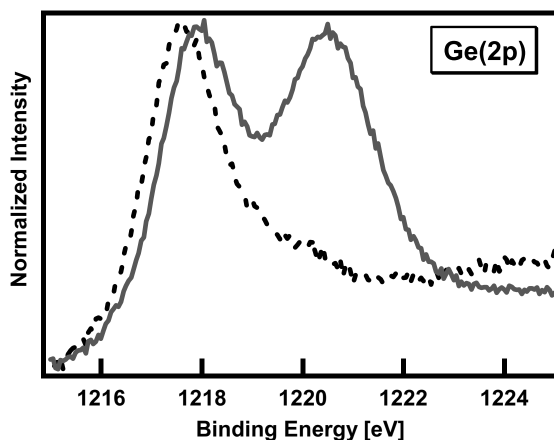

Fig. 9. The Ge(2p) region of the XPS spectrum of the 1-month-old Ge(1 1 1)–decyl (dashed line). The solid line shows spectra of the Ge(1 1 1)–GeO_2.

the Ge(1 1 1)–alkyl surface, most likely when the unstable Ge–H surface was exposed to air. The SHG-RA shows that there is no change over a month period, thus the suboxide is not due to oxidation of the alkyl-terminated surface. The lack of oxide growth is attributed to the stability of the Ge–C bond and the compactness of the alkyl monolayer.

4. Conclusions

XPS and SHG measurements reveal that H- and Cl-terminated Ge(1 1 1) undergo oxidation in air on the timescale of minutes with H–Ge(1 1 1) being less stable in ambient than Cl–Ge(1 1 1). The instability of H- and Cl-termination explains why the SHG-RA at 800 nm appears to be insensitive to the chemical modification of the germanium surface. The similar electronegativity of Cl and O is consistent with the observed moderate change in the SHG-RA upon Cl-termination. The oxide thickness growth kinetics are logarithmic both on 'H–Ge(1 1 1)' and 'Cl–Ge(1 1 1)', also characteristic of the ambient oxidation of Si(1 0 0)–H and Si(1 1 1)–H. S- and alkyl-termination significantly modify the interface non-linear optical response, as revealed by SHG-RA at 800 nm. The alkyl- and S-terminations are significantly more stable against oxidation.

Acknowledgements

The authors would like to thank to Catherine Faler for the preparation of the decyl-terminated germanium surface. The authors acknowledge the generous support of the NSF (CHE-9734273). EB acknowledges the NSF for a CAREER award in support of this research. DHW and HY acknowledge NSF-NER (ECS-0102912).

References

[1] J. Bardeen, W.H. Brattain, The transistor, a semiconductor triode, Phys. Rev. 74 (1948) 230–231.
[2] C. Kittel, Introduction to Solid State Physics, sixth ed., John Wiley and Sons, New York, 1986.
[3] P. Balk, in: P. Balk (Ed.), The Si–SiO_2 System, vol. 32, Elsevier, Amsterdam, 1988, pp. 2–20.
[4] J. Oh, J.C. Campbell, S.G. Thomas, S. Bharatan, R. Thoma, C. Jasper, R.E. Jones, T.E. Zirkle, Interdigitated Ge p-i-n photodetectors fabricated on a Si substrate using graded SiGe buffer layers, IEEE J. Quant. Electron. 38 (2002) 1238–1241.
[5] T. Deegan, G. Hughes, An X-ray photoelectron spectroscopy study of the HF etching of native oxides on Ge(1 1 1) and Ge(1 0 0) surfaces, Appl. Surf. Sci. 123 (1998) 66–70.
[6] Z.H. Lu, Air-stable Cl-terminated Ge(1 1 1), Appl. Phys. Lett. 68 (1996) 520–522.
[7] G.W. Anderson, M.C. Hanf, P.R. Norton, Z.H. Lu, M.J. Graham, The S-passivation of Ge(1 0 0)-(1 × 1), Appl. Phys. Lett. 66 (1995) 1123–1125.
[8] P.F. Lyman, O. Sakata, D.L. Marasco, T.L. Lee, K.D. Breneman, D.T. Keane, M.J. Bedzyk, Structure of a passivated Ge surface prepared from aqueous solution, Surf. Sci. 462 (2000) L594–L598.
[9] K. Choi, J.M. Buriak, Hydrogermylation of alkenes and alkynes on hydride-terminated Ge(1 0 0) surfaces, Langmuir 16 (2000) 7737–7741.
[10] S.M. Han, W.R. Ashurt, C. Carraro, R. Maboudian, Formation of alkanethiol monolayer on Ge(1 1 1), J. Am. Chem. Soc. 123 (2001) 2422–2425.
[11] J.L. He, Z.H. Lu, S.A. Mitchell, D.D.M. Wayner, Self-assembly of alkyl monolayers on Ge(1 1 1), J. Am. Chem. Soc. 120 (1998) 2660–2661.
[12] R. Boukherroub, S. Morin, F. Bensebaa, D.D.M. Wayner, New synthetic routes to alkyl monolayers on the Si(1 1 1) surface, Langmuir 15 (1999) 3831–3835.
[13] A. Bansal, X.L. Li, I. Lauermann, N.S. Lewis, S.I. Yi, W.H. Weinberg, Alkylation of Si surfaces using a two-step halogenation Grignard route, J. Am. Chem. Soc. 118 (1996) 7225–7226.
[14] R.L. Cicero, M.R. Linford, C.E.D. Chidsey, Photoreactivity of unsaturated compounds with hydrogen-terminated silicon(1 1 1), Langmuir 16 (2000) 5688–5695.
[15] R. Boukherroub, D.D.M. Wayner, Controlled functionalization and multistep chemical manipulation of covalently modified Si(1 1 1) surfaces, J. Am. Chem. Soc. 121 (1999) 11513–11515.
[16] A.B. Sieval, A.L. Demirel, J.W.M. Nissink, M.R. Linford, J.H. van der Maas, W.H. de Jeu, H. Zuilhof, E.J.R. Sudholter, Highly stable Si–C linked functionalized monolayers on the silicon (1 0 0) surface, Langmuir 14 (1998) 1759–1768.
[17] P. Wagner, S. Nock, J.A. Spudich, W.D. Volkmuth, S. Chu, R.L. Cicero, C.P. Wade, M.R. Linford, C.E.D. Chidsey, Bioreactive self-assembled monolayers on hydrogen-passivated Si(1 1 1) as a new class of atomically flat substrates for biological scanning probe microscopy, J. Struct. Biol. 119 (1997) 189–201.
[18] X.Y. Zhu, V. Boiadjiev, J.A. Mulder, R.P. Hsung, R.C. Major, Molecular assemblies on silicon surfaces via Si–O linkages, Langmuir 16 (2000) 6766–6772.

[19] G. Lüpke, Characterization of semiconductor interfaces by second-harmonic generation, Surf. Sci. Rep. 35 (1999) 75–161.
[20] J.I. Dadap, P.T. Wilson, M.H. Anderson, M.C. Downer, Femtosecond carrier-induced screening of dc electric-field-induced second-harmonic generation at the Si(001)–SiO_2 interface, Opt. Lett. 22 (1997) 901–903.
[21] J. Fang, G.P. Li, Detection of gate oxide charge trapping by second-harmonic generation, Appl. Phys. Lett. 75 (1999) 3506–3508.
[22] W. Daum, H.J. Krause, U. Reichel, H. Ibach, Identification of strained silicon layers at silicon–silica interfaces and clean silicon surfaces by nonlinear optical spectroscopy, Phys. Rev. Lett. 71 (1993) 1234–1237.
[23] J.I. Dadap, B. Doris, Q. Deng, M.C. Downer, J.K. Lowell, A.C. Diebold, Randomly oriented Angstrom-scale microroughness at the Si(100) SiO_2 interface probed by optical 2nd-harmonic generation, Appl. Phys. Lett. 64 (1994) 2139–2141.
[24] S.A. Mitchell, R. Boukherroub, S. Anderson, Second harmonic generation at chemically modified Si(111) surfaces, J. Phys. Chem. B 104 (2000) 7668–7676.
[25] S.A. Mitchell, M. Mehendale, D.M. Villeneuve, R. Boukherroub, Second harmonic generation spectroscopy of chemically modified Si(111) surfaces, Surf. Sci. 488 (2001) 367–378.
[26] D. Bodlaki, E. Borguet, The dynamics and second order nonlinear susceptibility of photo excited carrier at Si(111) interfaces, J. Appl. Phys., in press.
[27] N. Bloembergen, R.K. Chang, S.S. Jha, C.H. Lee, Optical second-harmonic generation in reflection from media with inversion symmetry, Phys. Rev. 174 (1968) 813–822.
[28] D. Guidotti, T.A. Driscoll, H.J. Gerritsen, Second harmonic generation in centro-symmetric semiconductors, Solid State Commun. 46 (1983) 337–340.
[29] J.A. Litwin, J.E. Sipe, H.M. Van Driel, Picosecond and nanosecond laser-induced second-harmonic generation from centrosymmetric semiconductors, Phys. Rev. B 31 (1985) 5543–5546.
[30] O.A. Aktsipetrov, I.M. Baranova, Y.A. Il'inskii, Surface contribution to the generation of the reflected second-harmonic light for centrosymmetric semiconductors, Sov. Phys. JETP 64 (1986) 167–173.
[31] J.E. Sipe, D.L. Moss, H.M. van Driel, Phenomenological theory of optical second- and third-harmonic generation from cubic centrosymmetric crystals, Phys. Rev. B 35 (1987) 1129–1141.
[32] V. Mizrahi, J.E. Sipe, Phenomenological treatment of surface second-harmonic generation, J. Opt. Soc. Am. B: Opt. Phys. 5 (1988) 660–667.
[33] G. Lüpke, D.J. Bottomley, H.M. van Driel, Second- and third-harmonic generation from cubic centrosymmetric crystals with vicinal faces: phenomenological theory and experiment, J. Opt. Soc. Am. B 11 (1994) 33–44.
[34] M.C. Downer, B.S. Mendoza, V.I. Gavrilenko, Optical second harmonic spectroscopy of semiconductor surfaces: advances in microscopic understanding, Surf. Interface Anal. 31 (2001) 966–986.
[35] V. Fomenko, D. Bodlaki, C. Faler, E. Borguet, Second-harmonic generation from chemically-modified Ge(111) interfaces, J. Chem. Phys. 116 (2002) 6745–6754.
[36] D. Bodlaki, E. Freysz, E. Borguet, Infrared second harmonic spectroscopy of germanium interfaces, J. Chem. Phys. 119 (2003) 3958–3962.
[37] D. Bodlaki, E. Borguet, Picosecond infrared optical parametric amplifier for nonlinear interface spectroscopy, Rev. Sci. Instrum. 71 (2000) 4050–4056.
[38] V. Fomenko, J.F. Lami, E. Borguet, Non-quadratic second harmonic generation from semiconductor–oxide interfaces, Phys. Rev. B 63 (2001) 121316.
[39] H. Yamamoto, R.A. Butera, Y. Gu, D.H. Waldeck, Characterization of the surface to thiol bonding in self-assembled monolayer films of $C_{12}H_{25}SH$ on InP(100) by angle-resolved X-ray photoelectron spectroscopy, Langmuir 15 (1999) 8640–8644.
[40] J.I. Dadap, Z. Xu, X.F. Hu, M.C. Downer, N.M. Russell, J.G. Ekerdt, O.A. Aktsipetrov, Second-harmonic spectroscopy of a Si(001) surface during calibrated variations in temperature and hydrogen coverage, Phys. Rev. B 56 (1997) 13367–13379.
[41] G. Erley, R. Butz, W. Daum, Second-harmonic spectroscopy of interband excitations at the interfaces of strained S(100)–$Si_{0.85}Ge_{0.15}$–SiO_2 heterostructures, Phys. Rev. B 59 (1999) 2915–2926.
[42] D.R. Lide (Ed.), CRC Handbook, 1998, pp. 9–74.
[43] D. Bodlaki, V. Fomenko, E. Borguet, Photoreactivity of Si(111)–H in ambient, in preparation.
[44] D. Bodlaki, V. Fomenko, E. Borguet, Ambient oxidation of Si(111)–H, in preparation.
[45] K. Prabhakaran, T. Ogino, Oxidation of Ge(100) and Ge(111) surfaces—an UPS and XPS study, Surf. Sci. 325 (1995) 263–271.
[46] D. Gräf, M. Grundner, R. Schulz, L. Mühlhoff, Oxidation of HF treated Si wafer surfaces in air, J. Appl. Phys. 68 (1990) 5155–5161.
[47] D. Briggs, M.P. Seah (Eds.), Practical Surface Analysis, vol. 1, John Wiley & Sons, Salle+Sauerlander, Chichester, 1990.
[48] R.J. Archer, Optical measurement of film growth on silicon and germanium surfaces in room air, J. Electrochem. Soc. 104 (1957) 619.
[49] M.R. Houston, R. Maboudian, Stability of ammonium fluoride-treated Si(100), J. Appl. Phys. 78 (1995) 3801.
[50] M. Morita, T. Ohmi, E. Hasegwa, M. Kawakami, K. Suma, Control factor of native oxide growth on silicon in air or in ultrapure water, Appl. Phys. Lett. 56 (1989) 562–564.
[51] D. Gräf, M. Grundner, R. Schulz, Reaction of water with hydrofluoric acid treated silicon(111) and (100) surfaces, J. Vac. Sci. Technol. A 7 (1989) 808–813.